

CLIMBING A LEGENDRIAN MOUNTAIN RANGE WITHOUT STABILIZATION

DOUGLAS J. LAFOUNTAIN AND WILLIAM W. MENASCO

ABSTRACT. In [EH], Etnyre and Honda provide a classification of the Legendrian isotopy classes for a $(2, 3)$ -cable of a $(2, 3)$ -torus knot as it is embedded in S^3 with the standard contact structure. To do this, they use the theory of convex surfaces in a tight contact structure. Their classification takes the visual form of a mountain range formed from points having values of (r, tb) , where r is the rotation number and tb is the Thurston-Bennequin number. In [M3] and [MM], the two Legendrian classes at $(r, tb) = (2, 5)$ are realized as rectangular braided diagrams, and are seen to be related by an elementary negative flype. In this note, we first prove directly that the rectangular braided diagrams in [M3] do represent the two Legendrian classes at $(r, tb) = (2, 5)$. In the process we provide a way to visualize convex tori peripheral to positive torus knots in S^3 . We then complete the realization of the Legendrian isotopy classes for a $(2, 3)$ -cable of a $(2, 3)$ -torus knot, describing how to construct a Legendrian representative of arbitrary (r, tb) value. We also analyze the relationships amongst these representatives, and this analysis yields an enhanced Legendrian mountain range where elementary negative flypes allow us to move toward the maximal tb value without having to use Legendrian stabilization. Thus, we obtain for this particular cable knot type a *Legendrian Markov Theorem without Stabilization* (LMTWS). Finally, the enhanced Legendrian mountain range and associated LMTWS determines the transverse classes of a $(2, 3)$ -cable of a $(2, 3)$ -torus knot along with an associated *transverse Markov Theorem without Stabilization* (TMTWS). Specifically, negative braid destabilizations and an elementary negative flype are sufficient to move toward maximal self-linking number in the transverse classes of a $(2, 3)$ -cable of a $(2, 3)$ -torus knot.

1. INTRODUCTION

Consider S^3 , which can be seen as the one-point compactification of \mathbb{R}^3 . In this context, the standard contact structure on S^3 can be thought of as the closure of the standard contact structure on \mathbb{R}^3 , given in cylindrical coordinates as the kernel of the 1-form $dz + \rho^2 d\theta$. We denote this standard contact structure by ξ_{sym} ; it is depicted on the left in Figure 1. ξ_{sym} is a *tight* contact structure, meaning there is no embedded disc that is tangent to the contact structure along its boundary. Given a topological knot type \mathcal{K} , we can restrict ourselves to look at representatives that are everywhere tangent to ξ_{sym} . These are called Legendrian knots, and we say that two Legendrian knots are Legendrian isotopic if they can be connected by a 1-parameter family of Legendrian knots. Similarly, we can restrict ourselves to look at representatives that are everywhere transverse to ξ_{sym} . These are called transverse, or transversal, knots, and we say that two transverse knots are transversally isotopic if they can be connected by a 1-parameter family of transverse knots.

Both Legendrian and transverse knots have classical invariants, besides the topological knot type, that are preserved under Legendrian and transverse isotopies, respectively.

Date: April 8, 2019.

Key words and phrases. Contact structures, convex surfaces, braids, Legendrian, transverse.
 2000 *Mathematics Subject Classification.* Primary 57M25, 57R17; Secondary 57M50.

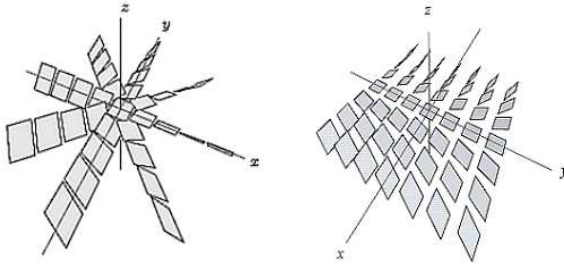


FIGURE 1. On the left are the contact planes for ξ_{sym} when $z = 0$; the planes for arbitrary z -value are similar. On the right is ξ_{std} . This figure is the work of S. Schonenberger, and is taken from [E1].

The Legendrian invariants are the rotation number, denoted by r , and the Thurston-Bennequin number, denoted by tb . The transverse invariant is the self-linking number, denoted by sl . A thorough discussion of these invariants, as well as general background to Legendrian and transverse knots, is provided in the excellent survey article by Etnyre found in [E1]. In this note, we will focus primarily on Legendrian knots, leaving a discussion of transverse knots to the final section.

For any topological knot type \mathcal{K} , one can represent the Legendrian isotopy classes as points on a two-dimensional grid, where the two coordinates are given by the values of (r, tb) for that class. For \mathcal{K} , there is a maximum value for the Thurston-Bennequin number, and thus this representation takes the shape of a *mountain range* (See Figure 2). If there are multiple isotopy classes having the same value of (r, tb) , this can be represented by drawing circles around the central point, one for each multiple isotopy class. The Legendrian mountain range for a $(2, 3)$ -cable of a $(2, 3)$ -torus knot is shown in Figure 2, and was established in [EH]. Note that the mountain range is symmetric about the $r = 0$ axis. This is true for any Legendrian mountain range. A blue arrow that goes down and to the left represents Legendrian negative stabilization, while a red arrow that goes down and to the right represents Legendrian positive stabilization. In the front projection of a Legendrian knot placed in the contact structure given by the kernel of $dz + xdy$ (which we call ξ_{std} , shown on the right in Figure 1), a negative stabilization is the addition of two up cusps, while a positive stabilization is the addition of two down cusps. See Figure 3, where positive stabilization is denoted by S_+ , negative stabilization by S_- . The reverse of positive (negative) stabilization (that is, the elimination of two consecutive down (up) cusps) is positive (negative) destabilization.

A topological knot type \mathcal{K} is said to be *Legendrian simple* if all of its Legendrian isotopy classes can be distinguished by the ordered pair (r, tb) . It is known that not all knot types are Legendrian simple; in particular, a consequence of Figure 2 is that a $(2, 3)$ -cable of a $(2, 3)$ -torus knot is not Legendrian simple.

There are some results proved in [EH] that are not immediately evident from the mountain range shown in Figure 2. We thus have included Figure 4, which shows the same mountain range as in Figure 2, but now with an extra z -dimension to clarify the relationships between the different isotopy classes that were established in [EH]. In particular, the outer circle at $(r, tb) = (2, 5)$ in Figure 2 is a gray circle at the point $(r, tb, z) = (2, 5, 1)$ in Figure 4. Note that this isotopy class does not Legendrian destabilize. Thus, in order to move from this isotopy class to an isotopy class of maximal tb , we must first stabilize down to

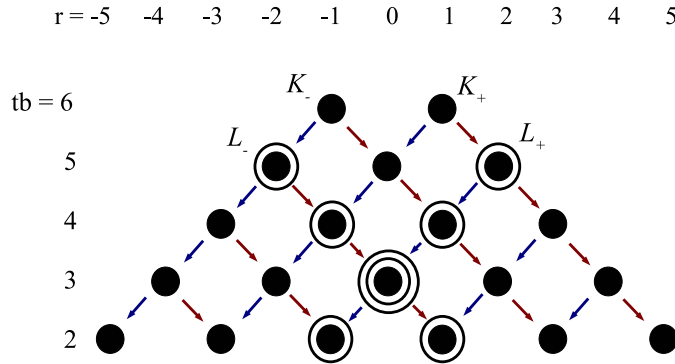


FIGURE 2. The Legendrian mountain range for a $(2,3)$ -cable of a $(2,3)$ -torus knot. A central dot and concentric circles represent multiple isotopy classes at a given value of (r, tb) . Blue arrows represent Legendrian negative stabilization; red arrows represent Legendrian positive stabilization. K_+ , K_- , L_+ , and L_- are defined in [EH].

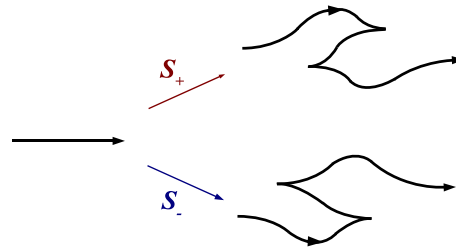


FIGURE 3. Legendrian positive stabilization is indicated as S_+ ; negative stabilization is indicated as S_- . Both stabilizations are as seen in the front projection of a Legendrian knot in ξ_{std} .

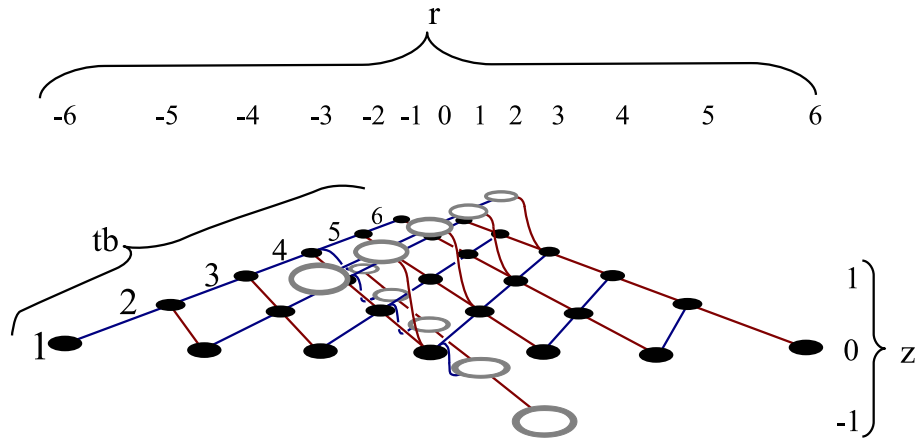


FIGURE 4. The Legendrian mountain range for a $(2,3)$ -cable of a $(2,3)$ -torus knot, with an extra z dimension added. Black dots and gray circles represent distinct isotopy classes; blue lines represent Legendrian negative (de)stabilization; red lines indicate Legendrian positive (de)stabilization.

the plane $z = 0$, and then destabilize to an isotopy class with maximal tb value. Thus the Figure 4 presentation of the mountain range requires us to use stabilization if we are to move from an arbitrary isotopy class toward the maximal value of tb .

The goal of this note is to provide a way to visualize representatives in the isotopy classes in Figure 2, as well as describing how one can move around in the mountain range from one representative to another. In particular, we want to show how to move toward maximal tb value without using stabilization. Our results will be dependent upon the work of Etnyre and Honda in [EH], and will expand upon the work of Matsuda and the second author in [M3] and [MM]. In order to accomplish our goal, justification will be provided to show that our examples are indeed those of the mountain range. In particular, we will need to connect two seemingly different embeddings of tori in S^3 , namely *standardly tiled tori*, on which the knots in [M3] reside; and *convex tori*, on which the knots in [EH] reside. We do this in Section 2, showing there is a natural way to make standardly tiled tori into convex tori while preserving topological information. In Section 3, we explicitly describe the knots and moves seen in the Legendrian mountain range in Figure 2, and provide an enhanced Legendrian mountain range where elementary negative flypes are used to connect central dots to concentric circles at the same value of (r, tb) . Finally, in Section 4, we discuss how a Legendrian mountain range yields a way of seeing the transverse isotopy classes of a knot type, in particular in the case of a $(2, 3)$ -cable of a $(2, 3)$ -torus knot. This yields a transverse Markov Theorem without Stabilization for the transverse isotopy classes of this particular knot type; specifically, given an arbitrary transverse isotopy class, negative braid destabilizations and an elementary negative flype are sufficient to move to the class with maximal sl .

Because we are interested in a particular knot type, for ease of notation the topological knot type of a $(2, 3)$ -torus knot will be denoted by \mathcal{K} , and the topological knot type of a $(2, 3)$ -cable of a $(2, 3)$ -torus knot will be denoted by $\mathcal{K}_{(2,3)}$. The torus peripheral to \mathcal{K} on which $\mathcal{K}_{(2,3)}$ resides will be denoted by \mathcal{T} .

2. CONVEX TORI, STANDARD TILINGS, AND RECTANGULAR DIAGRAMS

2.1. Convex tori. The Legendrian knots in [EH] are knots that reside on convex surfaces. We thus will need to review the definition and properties of convex surfaces found in [G], [H], and [K].

Definition 2.1. A surface in (S^3, ξ_{sym}) is said to be *convex* if there exists a vector field that is everywhere transverse to the surface, and whose flow preserves the contact structure. This vector field is called a *contact vector field*.

We need another definition, however, to illuminate the useful properties of convex surfaces.

Definition 2.2. Let \mathcal{F} be a singular foliation on a closed orientable surface F . Then a disjoint union of simple closed curves $\Gamma \subset F$ *divides* \mathcal{F} if Γ satisfies the following properties:

1. Γ divides F into two parts F^+ and F^- such that $\Gamma = \partial F^+ = -\partial F^-$.
2. Γ is everywhere transverse to the foliation \mathcal{F} .
3. There is a flow Y and a volume form ω on F such that:
 - a. Y represents \mathcal{F} .
 - b. $L_Y \omega > 0$ on F^+ and < 0 on F^- .
 - c. $Y|_{F^+}$ goes outward along ∂F^+ .

Γ is called a *dividing set*.

For a surface in (S^3, ξ_{sym}) , its *characteristic foliation* is the foliation induced by the contact structure. The following special case of a theorem in [G] begins to connect convex surfaces with dividing sets:

Theorem 2.3 (Giroux). *A closed orientable surface F embedded in (S^3, ξ_{sym}) is convex if and only if there exists a dividing set Γ for the characteristic foliation on F .*

The following theorem, known as Giroux's Flexibility Theorem, effectively says that it is the dividing set that determines the geometry of ξ_{sym} near F :

Theorem 2.4 (Giroux). *Let F be a closed convex surface, with a contact vector field v . Let Γ be the dividing set for the characteristic foliation, and let \mathcal{F} be another singular foliation on F that is divided by Γ . Then there is an isotopy ϕ_t of F so that $\phi_0(F) = F$, the characteristic foliation of $\phi_1(F)$ is \mathcal{F} , ϕ_t keeps Γ fixed for all t , and $\phi_t(F)$ is transverse to v for all t .*

There is a corresponding theorem proved in [H] for a compact convex surface with Legendrian boundary.

Remark 2.5. Another observation due to Giroux is that in a tight contact structure, no dividing curve on a closed convex surface can bound a disc on the surface unless the surface is the 2-sphere. See [H].

If the convex surface is a torus, we can now give a description of the characteristic foliation induced by the contact structure. In particular, by Definition 2.2, Theorem 2.3, and Remark 2.5 there will be an even number of parallel, homotopically non-trivial simple closed *dividing curves*. These will be transverse to the characteristic foliation. By Theorem 2.4, we may assume that a parallel push-off of these curves gives an even number of parallel Legendrian curves that are actually curves of singularities, meaning all along these curves, the tangent plane to the torus and the contact plane coincide. We will call these the *Legendrian divides*. The rest of the foliation will be given by a 1-parameter family of curves that intersect the Legendrian divides at singular points. This 1-parameter family will be called *Legendrian rulings*. By part 3 of Definition 2.2, as we move along a Legendrian ruling, it will alternately intersect positive and negative singularities.

The knots in Figure 2, in the work of Etnyre and Honda, are either Legendrian rulings or Legendrian divides on convex tori. For these convex tori in [EH], denoted by \mathcal{T} , two coordinate systems are used. One coordinate system, denoted by $\mathcal{C}_{\mathcal{K}}$, has a meridian of \mathcal{T} having slope 0 and the preferred longitude of \mathcal{T} having slope ∞ . The other coordinate system on \mathcal{T} , denoted by $\mathcal{C}'_{\mathcal{K}}$, has a meridian having slope 0. The curve having slope ∞ is found in the following manner: Take the torus, peripheral to the unknot, on which \mathcal{K} resides, and call it T_0 . Since \mathcal{T} is peripheral to a representative of \mathcal{K} on T_0 , \mathcal{T} will intersect T_0 in two parallel curves. The slope of these curves on \mathcal{T} is given the value ∞ in $\mathcal{C}'_{\mathcal{K}}$. As shown in [EH], L_+ (the outer circle at (2, 5) in Figure 2) is a Legendrian ruling on a convex torus that has two Legendrian divides of slope $-\frac{2}{11}$ in $\mathcal{C}'_{\mathcal{K}}$.

2.2. Standard tilings and rectangular diagrams. We now want to connect convex tori and Legendrian knots to the work of Menasco and Matsuda on standardly tiled tori and transverse knots. We review definitions found in [M1] and [M3]. Consider $(\mathbb{R}^3, \{z - axis\}) \subset (S^3, \mathbf{A})$, where \mathbf{A} is the axis of a transverse braid, $S^3 = \mathbb{R}^3 \cup \infty$, and

$\mathbf{A} = \{z - \text{axis}\} \cup \infty$. In our case, this transverse braid will lie on a torus. Let (ρ, θ, z) be the cylindrical coordinate system. We denote the braid fibration by $\mathbf{H} = \{H_\theta \mid 0 \leq \theta < 2\pi\}$. This will induce a singular braid foliation on the surface of the torus. Specifically, as discussed in [BF], the torus will intersect each half-plane H_θ , and there will be only finitely many values of θ where a tangent plane to the torus actually resides in H_θ . These singular points may be assumed to be at distinct values of θ , and are saddle singularities. The non-singular leaves will be either arcs that have their endpoints on \mathbf{A} , which are called b-arcs, or circles, which are called c-circles. We will be concerned with the case where all non-singular leaves are b-arcs. In this case, singular leaves will be where two b-arcs intersect. Singular points may be assigned a parity, being positive when the orientation of the torus points in the direction of increasing θ , and being negative when otherwise. We may also assume the torus intersects \mathbf{A} in finitely many points, which will be called vertices on our foliation. Vertices are assigned a parity, being positive when the orientation of the torus agrees with the direction of the braid axis, and being negative otherwise. The valence of a vertex is the number of singularities adjacent to it via singular b-arcs. A *standard tiling* is where each vertex has valence four; in this case, for a given vertex, the parities of its adjacent singularities alternate between positive and negative as one proceeds cyclically through θ . A tile consists of a singular leaf, the vertices adjacent to that leaf, along with non-singular b-arcs occurring just before and after the singularity in the θ -ordering of the leaves of the foliation. See Figure 7, where each tile is a square bounded by gray arcs, and each negative singularity is the intersection of a green and blue arc, while a green and red arc intersection indicates a positive singularity.

In [M3], a particular standardly tiled torus, and transverse braid on that tiling, are studied. We review how to define both this torus and knot of interest. We will call the standardly tiled torus $\widehat{\mathcal{T}}$, the knot that forms its core, \widehat{K} , and the knot on the torus, $\widehat{K}_{(2,3)}$. To see how to view $\widehat{\mathcal{T}}$, we first construct the solid torus for which $\widehat{\mathcal{T}}$ is the boundary. This solid torus can be represented as a rectangular block diagram, as described in [M3]. In particular, take a collection of discs of radius one whose centers are on the braid axis and which are parallel to the xy -plane. We then attach to each disc a unique rectangular-shaped block whose bottom edge is on the boundary of the disc. The top edges of the blocks are also attached to discs in a one-to-one fashion. We do this so that we have a collection of discs, $\{D_1, D_2, \dots, D_m\}$, and blocks, $\{R_1, R_2, \dots, R_m\}$, which deformation retracts onto a closed braid, particularly a positive trefoil \widehat{K} . A regular neighborhood of the block-disc collection forms a solid torus whose boundary is $\widehat{\mathcal{T}}$. Negative singularities occur just to the left of the left edges of blocks, while positive singularities occur just to the right of the right edges of blocks. Negative vertices are just below the centers of the discs, while positive vertices are just above the centers of the discs. A rectangular block diagram for \widehat{K} is shown in Figure 5. There the blocks are in light blue, the discs white. A salient feature is that the left side of a block shares the same angular position as the right side of a block below it. This implies that the negative singularity on $\widehat{\mathcal{T}}$ actually occurs before the positive singularity in the θ -ordering.

Our knot of interest, $\widehat{K}_{(2,3)} \in \mathcal{K}_{(2,3)}$, is a transverse braid on the surface of $\widehat{\mathcal{T}}$. We can visualize this braid as being superimposed on the rectangular block diagram of $\widehat{\mathcal{T}}$. This yields a braided rectangular diagram consisting of a collection of vertical and horizontal arcs, as defined in [M3] and [MM]. The braided rectangular diagram for $\widehat{K}_{(2,3)}$ is shown in Figure 6. Notice that $\widehat{K}_{(2,3)}$ has vertical arcs that go down along the front of the blocks,

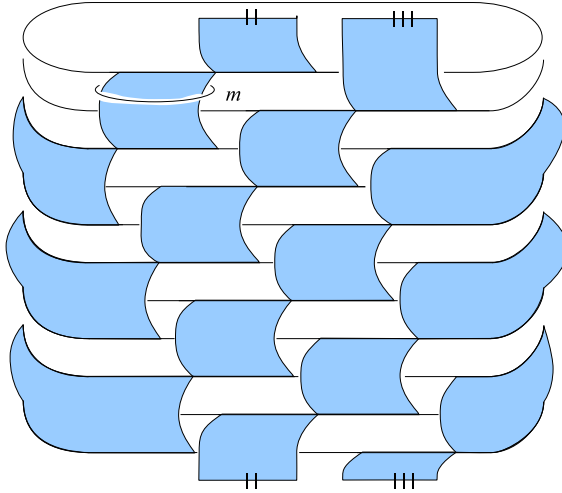


FIGURE 5. A rectangular block presentation for the positive trefoil \widehat{K} . Discs are in white, blocks are in light blue. The boundary of a regular neighborhood of this collection of blocks and discs forms the torus $\widehat{\mathcal{T}}$. A meridian curve of $\widehat{\mathcal{T}}$ is indicated by the letter m .

two blocks at a time, except for the one vertical arc in the upper left corner that passes behind one of the blocks. The vertical arcs passing in front of two blocks at a time should be understood as running between the negative singularity that comes from the left edge of the top block, and the positive singularity that comes from the right edge of the bottom block. It is clear that this knot has intersection number three with a meridian; by drawing the preferred longitude on the surface of $\widehat{\mathcal{T}}$, one can confirm that the knot has intersection number two with that longitude, and hence is a $(2, 3)$ -cabling.

We can now imagine taking the discs and increasing their radii to a large enough value r so that at the boundary of the discs, the contact planes are ϵ -close to being in the half planes H_θ . We then slightly tilt the blocks so that their sides are aligned with the contact planes at the large radius r . Taking a neighborhood of this new block-disc presentation will give a solid torus on whose boundary the elliptic singularities will be positive-negative pairs where the z -axis intersects the discs, and the hyperbolic singularities will be positive-negative pairs that occur on the edges of each of the blocks. The characteristic foliation is thus a standard tiling. We can do this while keeping the transverse isotopy class of the knot the same, and while maintaining the fact that the braid foliation is a standard tiling. We thus have the following lemma:

Lemma 2.6. *Suppose that the transverse braid $\widehat{K}_{(2,3)}$ lies on a standardly tiled torus $\widehat{\mathcal{T}}$, with the tiling induced by the braid fibration. Then we may assume that $\widehat{K}_{(2,3)}$ lies on a standardly tiled torus $\widehat{\mathcal{T}}$, where the characteristic foliation is also a standard tiling.*

On a tiling, we can define four graphs, $G_{\epsilon\delta}$, that consist of vertices of parity ϵ connected by edges that are in singular leaves of parity δ . For a standard tiling, the components of G_{++} and G_{--} form a collection of an even number of parallel, homotopically non-trivial simple closed curves on the torus [M1]. In Figure 7, we illustrate the tiling of $\widehat{\mathcal{T}}$ with G_{++} in red, G_{--} in blue, and $\widehat{K}_{(2,3)}$ in black. We have not distinguished between G_{-+} and G_{+-} ; both are green. Note that on $\widehat{\mathcal{T}}$, G_{++} and G_{--} both have just one component, a simple

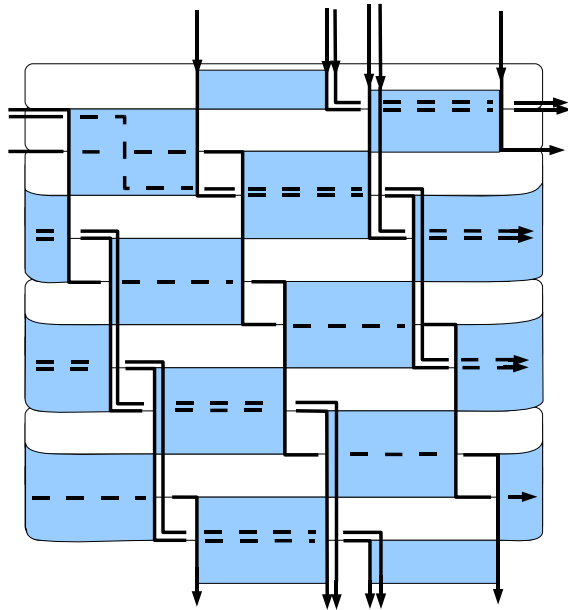


FIGURE 6. $\widehat{K}_{(2,3)}$ on the rectangular block diagram of $\widehat{\mathcal{T}}$. Vertical arcs going down the front of two consecutive blocks actually pass between the negative singularity that comes from the left edge of the top block, and the positive singularity that comes from the right edge of the bottom block.

closed loop. Note also that $\widehat{K}_{(2,3)}$ intersects G_{++} and G_{--} each once. In this figure, each box outlined in light gray is a tile, with corners being vertices, and a singularity in the center.

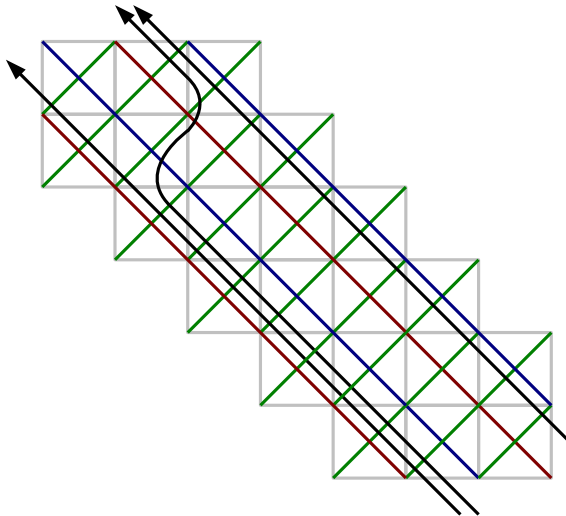


FIGURE 7. Each gray square represents a tile, with corners being vertices, and a singularity in the center. Shown in black is $\widehat{K}_{(2,3)}$. G_{++} is red, G_{--} is blue. In this figure, we have not distinguished between G_{-+} and G_{+-} ; both are green.

Now G_{++} and G_{--} are piecewise Legendrian curves. By a small isotopy of $\widehat{\mathcal{T}}$ near the braid axis, we may smooth out the corners and assume that G_{++} and G_{--} are Legendrian

curves. In Figure 8, we show G_{++} superimposed on the rectangular block presentation for $\widehat{\mathcal{T}}$. We have labelled the positive hyperbolic singularities with a red x, and the positive elliptic singularities with a red dot.

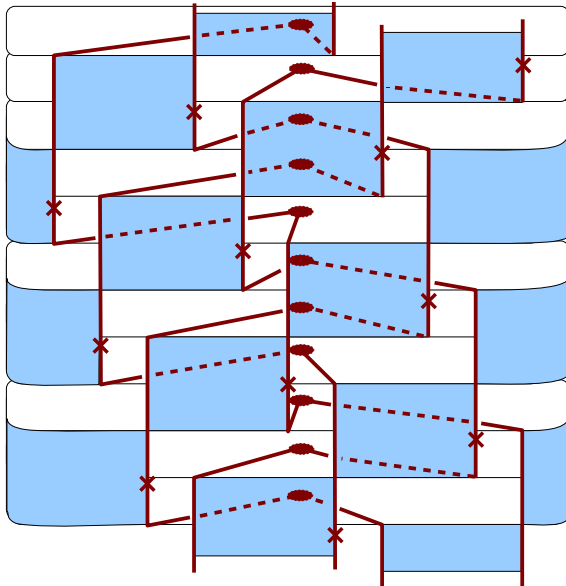


FIGURE 8. G_{++} superimposed on \mathcal{T} . Elliptic singularities are red dots; hyperbolic singularities are indicated by a red x.

If we compare Figure 8 with Figure 6, we can see that $\widehat{K}_{(2,3)}$ intersects G_{++} right after the occurrence of the vertical arc that lies behind one of the blocks, and we can arrange things so this is the only intersection. Similarly, if one imagines G_{--} on $\widehat{\mathcal{T}}$, the only intersection of $\widehat{K}_{(2,3)}$ with G_{--} occurs just before the occurrence of that same vertical arc. This will be important later. Now in the coordinate system $\mathcal{C}'_{\mathcal{K}}$, G_{++} intersects each meridian curve algebraically twice. Moreover, the slope ∞ longitude intersects the top right corner of each block, and thus intersects G_{++} once for each block. These intersections are algebraically negative. Since there are eleven blocks, the slope of G_{++} in $\mathcal{C}'_{\mathcal{K}}$ is $-\frac{2}{11}$.

2.3. Making standardly tiled tori into convex tori. We now show how to make $\widehat{\mathcal{T}}$ convex. In particular, we have the following proposition.

Proposition 2.7. *Suppose $\widehat{\mathcal{T}}$ has a standard tiling that is the characteristic foliation. Then we can isotop $\widehat{\mathcal{T}}$, rel G_{++} and G_{--} , so that the resulting torus, \mathcal{T} , is convex, and the components of G_{++} and G_{--} are the Legendrian divides.*

Proof. The idea is to mimic a proof of Giroux Elimination, which says that adjacent hyperbolic and elliptic singularities of like sign on a surface can be removed. This is stated as Lemma 4.7 in [E2] and is due to Giroux and Fuchs. The proof we mimic is outlined in Exercise 4.8 in [E2]. However, in contrast to Giroux Elimination, we do not want to remove the singularities, but rather want to create a line of singularities between them. To do this, we will look at a neighborhood of two singularities of like sign on $\widehat{\mathcal{T}}$, and then look at a diffeomorphic neighborhood in $(\mathbb{R}^3, \xi_{std})$. We then show that we can isotop the surface in this neighborhood so that the foliation has a line of singularities between the

two original singularities, and in such a way that no other singularities are introduced. We then pull back to (S^3, ξ_{sym}) , and work our way around the components of G_{++} and G_{--} to complete the isotopy. Below we give the technical details.

Choose a pair of adjacent elliptic and hyperbolic singularities along G_{++} , and call them a and b . The characteristic foliation of $\widehat{\mathcal{T}}$ in an open neighborhood containing a and b looks like (1) in Figure 9. Now if we take a rectangle, R , and place it in $(\mathbb{R}^3, \xi_{std})$ in the xy -plane so that the y -axis bisects it lengthwise, we can then deform R to obtain a foliation that looks like the one in Figure 9, part (1). In particular, split R into five sections along the y -axis, so that the first and fifth sections have the equation $z = -\epsilon x$ for some small $\epsilon > 0$, the third section has the equation $z = \epsilon x$, and the second and fourth sections smoothly connect the first to the third, and the third to the fifth, respectively. This R is shown in (2) in Figure 9, and its characteristic foliation is the same as (1). This can be seen by looking at the characteristic foliation induced on R by the contact structure ξ_{std} depicted in Figure 1.

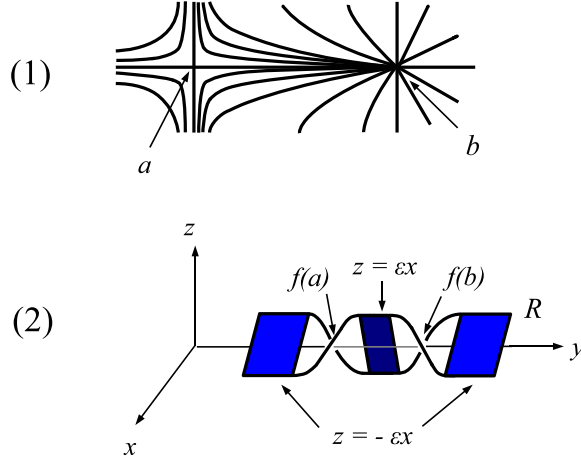


FIGURE 9. In (1) is shown the neighborhood of a hyperbolic-elliptic pair of positive singularities on the torus $\widehat{\mathcal{T}}$. In (2) is an embedding of a rectangle R in $(\mathbb{R}^3, \xi_{std})$; the characteristic foliation on this rectangle looks exactly like (1).

Now by Theorem 3.8 in [E2], there are neighborhoods of the segments connecting the two singularities in these two surfaces that are contactomorphic. Call the contactomorphism f , and the neighborhood in $(\mathbb{R}^3, \xi_{std})$, V . So the y -axis between $f(a)$ and $f(b)$ corresponds to the segment of G_{++} between a and b .

We now work on producing the appropriate isotopy of $R \cap V$ in $(\mathbb{R}^3, \xi_{std})$. To this end, take a copy of a closed $D^2 \times I$, and then take a closed 3-ball with radius that matches the radius of the D^2 . Cut this 3-ball along the equator, and glue the two halves to $D^2 \times 0$ and $D^2 \times 1$, respectively, and call it B . Then let $B_t, t \in [0, 2)$ be a collection of these B 's that satisfy the following conditions:

1. B_t is embedded in V for all t .
2. The y -axis forms the core of the $D^2 \times I$, and forms a radius of the halves of the 3-ball, for all of the B_t .
3. $f(a)$ is contained in $D^2 \times 0$ and $f(b)$ is contained in $D^2 \times 1$, for all of the B_t .
4. $\bigcup \partial B_t = B_0 - \{y\text{-axis between } f(a) \text{ and } f(b)\}$, and if $t < t'$, then $B_{t'} \subset \text{Int}(B_t)$.

5. For all B_t , $\gamma_t = \partial B_t \cap R$ crosses the planes $y = f(a)$ and $y = f(b)$ at $z = 0$. (This can actually be arranged previously in our construction of R .)

A picture of one of the B_t is shown in (1) in Figure 10.

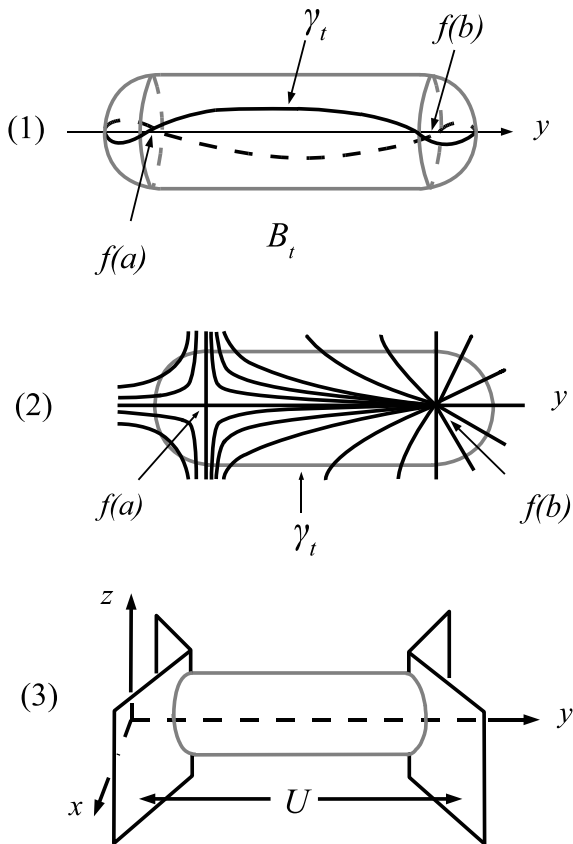


FIGURE 10. In (1), the surface ∂B_t for arbitrary t is indicated in gray. Its core is the y -axis between $f(a)$ and $f(b)$. In black is γ_t , which is the intersection of ∂B_t with the rectangle R . Note that γ_t has a y -value of $f(a)$ or $f(b)$ when $z = 0$. In (2), γ_t is in gray, and the figure indicates how γ_t is positioned in R with respect to the characteristic foliation. (3) shows the neighborhood U in which γ_t is transverse to the contact structure for all t .

If we look at γ_t in $R \cap V$, γ_t is tangent to the characteristic foliation at two points, but is transverse to the characteristic foliation in a neighborhood that contains all points in γ_t with y -values in $[f(a), f(b)]$. See (2) in Figure 10. Thus γ_t is transverse to the contact structure in this neighborhood. Moreover, there exists a $\delta > 0$ such that for all t , γ_t is transverse to the contact structure as long as its y -values are contained in the set $[-\delta|x| + f(a), \delta|x| + f(b)] = U$. A picture is given in (3) in Figure 10.

We will now show that we can isotop R inside $B_0 \cap U$, but leave it untouched outside. So fix t for the moment, and we look at γ_t with respect to the characteristic foliation on ∂B_t . Since in U , γ_t is transverse to the contact structure, it must be transverse to the characteristic foliation in $\partial B_t \cap U$. But $\{z = 0\} \cap \partial B_t$, which we call the equator, is also transverse to the characteristic foliation on $\partial B_t \cap U$. Furthermore, there are no singularities in the characteristic foliation of $\partial B_t \cap U$ near the equator. So in the set $\{f(a) \leq y \leq f(b)\}$, the

equator and γ_t form two disjoint bigons, one where $x > 0$ and one where $x < 0$, such that each point on the equator is connected to a unique point on γ_t via a unique leaf of the characteristic foliation on ∂B_t . Moreover, we can continue this one-to-one relationship between points on the equator and points on γ_t via leaves of the foliation in a neighborhood of $\{f(a) \leq y \leq f(b)\}$, which we call W_t . So we have the following picture in (1) of Figure 11.

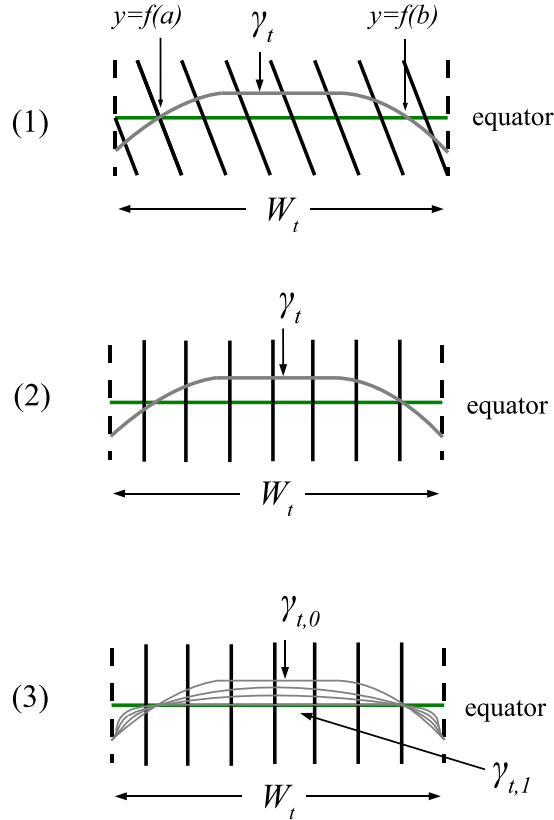


FIGURE 11. In (1), we have shown the neighborhood W_t on ∂B_t . γ_t is in gray, the characteristic foliation on ∂B_t is in black, and the equator is green. Points on the equator are connected to points on γ_t in a one-to-one fashion via leaves in the foliation. In (2) is the diffeomorphic situation where leaves are perpendicular to the equator. (3) shows the isotopy of γ_t to the equator. Note that γ_t remains fixed outside of W_t , and that $\gamma_{t,1}$ lies on the equator if and only if its y -values are in $[f(a), f(b)]$.

Now the leaves of the characteristic foliation will not be as straight as depicted in Figure 11, but the fact that they are parallel in $\{f(a) \leq y \leq f(b)\}$ and transverse to γ_t and the equator allow a diffeomorphism to the situation depicted in (2) of Figure 11.

From this figure it is evident that we can isotop γ_t in W_t via an isotopy $\gamma_{t,s}$ so that:

- i. $\gamma_t = \gamma_{t,0}$.
- ii. $\gamma_{t,1}$ is the equator for y -values in $[f(a), f(b)]$ and is not the equator for other y -values in W_t .
- iii. For each $s \in [0, 1]$, $\gamma_{t,s}$ only intersects the equator at $y = f(a)$ and $y = f(b)$.

- iv. For each s , $\gamma_{t,s}$ is transverse to the characteristic foliation on ∂B_t .
- v. $\gamma_{t,s} = \gamma_t$ outside of W_t for all s .

A picture of the isotopy is given in (3) of Figure 11. So now note that γ_t varies smoothly in the variable t , the foliation of ∂B_t varies smoothly in t , and we can arrange it so W_t varies smoothly in t . So we can construct our isotopies so that $\gamma_{t,s}$ varies smoothly in the variables t and s . In particular, the following describes a smooth isotopy of surfaces: Begin with $\Sigma_0 = f(\mathcal{T}) \cap V$. This surface will remain constant throughout the isotopy outside of B_0 , but inside B_0 we let, for $s \in [0, 1]$,

$$\Sigma_s \cap \partial B_t = \begin{cases} \gamma_{t,s} & \text{if } s \leq t \\ \gamma_{t,t} & \text{if } s > t \end{cases}$$

Now if there were a new singularity on some Σ_s off the y -axis, it would have to occur at a point on some $\gamma_{t',s'}$. But $\gamma_{t',s'}$ is transverse to the characteristic foliation on $\partial B_{t'} \cap U$, so this would induce a singularity at this point on $\partial B_{t'} \cap U$. However, there is no such singularity on $\partial B_{t'} \cap U$. Thus, Σ_1 has no new singularities off the y -axis. Moreover, by its construction, Σ_1 has a line of singularities along the y -axis between (and including) $f(a)$ and $f(b)$. This is because $\Sigma_1 \cap \partial B_t \cap \{f(a) \leq y \leq f(b)\} = \text{equator}$ for $t \in [1, 2]$, so that along the y -axis in $[f(a), f(b)]$, the tangent planes to Σ_1 are precisely the contact planes. The foliation of Σ_1 thus looks like that in Figure 12.

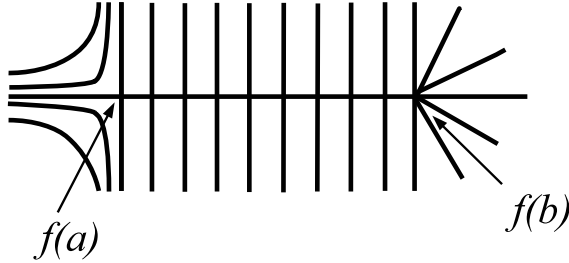


FIGURE 12. The line of singularities between $f(a)$ and $f(b)$ that occurs in the characteristic foliation after the isotopy. The endpoints of this line of singularities are a half-hyperbolic singularity and a half-elliptic singularity.

Notice that the y -axis remained fixed throughout the above isotopy. So we pull the above isotopy back to (S^3, ξ_{sym}) via f^{-1} , and the isotopy has been performed rel G_{++} . We then repeat this argument along G_{++} , noting that when we have half-elliptic or half-hyperbolic points, neighborhoods of these points can still be represented by a similar rectangle in $(\mathbb{R}^3, \xi_{std})$, and each γ_t will still be transverse to the characteristic foliation of R in a similar neighborhood U . So we can work our way around each component of G_{++} and G_{--} , and isotope $\widehat{\mathcal{T}}$ so that its foliation is now “double-combed” along G_{++} and G_{--} , with no singularities elsewhere. Moreover, any leaf coming off of G_{++} exits the neighborhood of G_{++} that was affected by the isotopies, and must again enter the neighborhood of G_{--} that was affected by the isotopies, and hence connect to G_{--} . The same is true for leaves coming off of G_{--} . Parallel push-offs of each component of G_{--} and G_{++} thus become dividing curves, and by Theorem 2.3 our resulting torus is convex, with G_{--} and G_{++} the Legendrian divides. \square

How will $\widehat{\mathcal{T}}$ be changed when we make it convex? In particular, how will Figure 8 change? The isotopy keeps G_{++} and G_{--} fixed, and only occurs in a neighborhood of G_{++} and

G_{--} . What this means is that \mathcal{T} will still be represented by a rectangular block diagram, with the blocks and discs now slightly warped as one moves along G_{++} and G_{--} . In particular, the disc will need to be isotoped as in (a) in Figure 13. In (b) of the same figure, we are viewing the z -axis as pointing toward us, and on the left is the boundary of a regular neighborhood of one of our original blocks before the isotopy. So we are viewing a meridional cross-section. The red dots on this block indicate G_{++} , and the blue dots indicate G_{--} . On the right in (b) is the block after the isotopy. Note that the red and blue dots have stayed fixed, since the isotopy keeps G_{++} and G_{--} fixed. The isotopy has changed the block in a neighborhood of G_{++} and G_{--} , however, and G_{++} and G_{--} are now actually curves of singularities. In Figure 14, we have put the discs and regular neighborhoods of our blocks together in a portion of the rectangular block presentation to show how the whole torus would change. In that figure, the curve of singularities coming from G_{++} is in red, and we have used two different shades of blue to indicate how the blocks have been warped. Note that the braid foliation on \mathcal{T} is still a standard tiling.

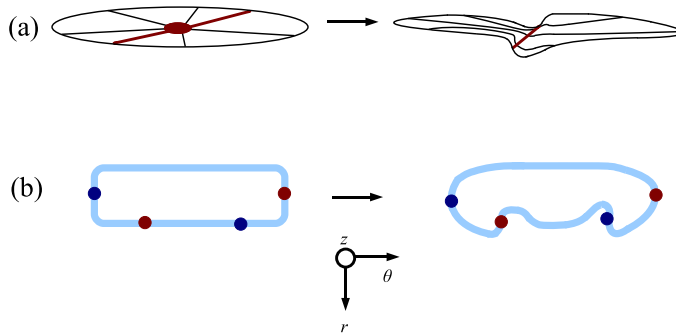


FIGURE 13. In (a) is shown how a disc is made convex. The disc has been isotoped in a neighborhood of G_{++} , resulting in a line of singularities where G_{++} was previously. In (b) a block is made convex. We are viewing the boundary of a neighborhood of the block, taking a meridional cross-section. G_{++} is in red, G_{--} is in blue, and the isotopy occurs in a neighborhood of these curves, resulting in curves of singularities.

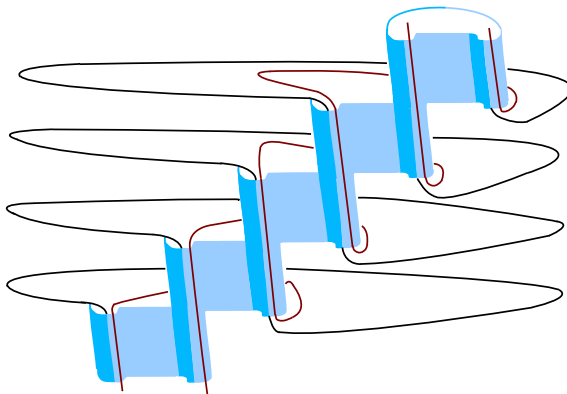


FIGURE 14. Shown is a rectangular block presentation for our convex torus, with warped discs and warped boundaries of neighborhoods of our blocks. The line of singularities corresponding to G_{++} is in red.

We note as an aside that we now have a way of describing the embedding of convex tori peripheral to both positive and negative torus knots. The above argument takes care of positive torus knots, since any positive torus knot can be seen as being a deformation retract of a rectangular block presentation that yields a standardly tiled torus. Negative torus knots can be seen as Legendrian torus knots on a cylinder peripheral to the z -axis; taking a torus peripheral to these knots yields a convex torus.

Getting back to our convex torus \mathcal{T} , we began with the slopes of G_{++} and G_{--} being $-\frac{2}{11}$ as measured in the coordinate system $\mathcal{C}'_{\mathcal{K}}$. In making the torus convex, these slopes remained $-\frac{2}{11}$. So we have a convex torus peripheral to a $(2, 3)$ -torus knot, such that the slope of the Legendrian divides is $-\frac{2}{11}$. Moreover, there are two Legendrian divides. This is the convex torus that is of interest in [EH]. The dividing curves are parallel push-offs of the two Legendrian divides. Furthermore, if we examine the proof of Proposition 2.7, one will note that the Legendrian rulings on \mathcal{T} are all parallel to the original graphs G_{+-} and G_{-+} on $\widehat{\mathcal{T}}$. Also, the portion of our knot that goes behind a block is parallel to these rulings between its two points of intersection with the Legendrian divides at the edges of the block.

Now by Giroux's Flexibility Theorem (Theorem 2.4), there is an isotopy of our convex torus such that the dividing curves remain fixed, but the resulting torus is still convex, with Legendrian rulings that are $(2, 3)$ -torus knots on our convex torus. Moreover, we can accomplish this isotopy in the following way. First imagine splitting our torus into two annuli bounded by the two Legendrian divides. One of the annuli contains the portion of our knot that is parallel to the current Legendrian rulings. We leave this annulus fixed. We isotope the other annulus using Giroux's Flexibility Theorem for surfaces with Legendrian boundary, so that the boundary of this annulus is still two curves of singularities, and the new rulings on the whole torus are $(2, 3)$ -torus knots. In this way the rulings will intersect each dividing curve once, and each Legendrian divide once. Because this isotopy kept the dividing curves fixed, we may still model our torus using a rectangular block presentation. The portion of our knot that went behind the block will join up with a ruling that runs parallel to the Legendrian divides throughout the rest of its support. Thus we would construct the braided rectangular diagram for our knot precisely the way we would construct the knot in [M3]. So the rectangular diagram in Figure 6 from [M3] is a rectangular diagram for the Legendrian representative of a $(2, 3)$ -cable of a $(2, 3)$ -torus knot that is a Legendrian ruling on a convex torus with Legendrian divides of slope $-\frac{2}{11}$. Moreover, using formulas for the rotation number and Thurston-Bennequin number established in [MM], one can calculate that for the diagram in Figure 6, $r = 2$ and $tb = 5$. Thus the diagram in Figure 6 is a braided rectangular diagram for L_+ in [EH].

3. REALIZING THE LEGENDRIAN MOUNTAIN RANGE

We have shown that the rectangular diagram in Figure 6 actually does represent L_+ in [EH], and in so doing have seen how to make a standardly tiled torus into a convex torus. In this section we will continue our analysis by showing how to represent all the knots in Figure 2 as braided rectangular diagrams. We therefore review some of the results in [MM] concerning the representation of Legendrian knots as braided rectangular diagrams. We first show in Figure 15 the moves that are sufficient to accomplish any Legendrian isotopy. Of particular importance for us will be the horizontal and vertical flips shown at

the bottom of the diagram.

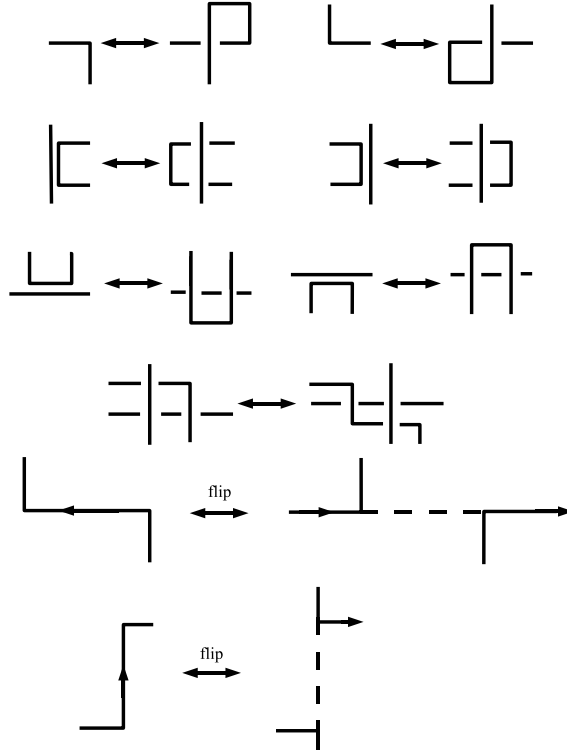


FIGURE 15. Reidemeister moves for Legendrian rectangular diagrams.

It will also be helpful to review the specific formulas for the rotation number and Thurston-Bennequin number that are established in [MM] and [M3] for the case of a braided rectangular diagram. To do this, first suppose we have a Legendrian knot K with a braided rectangular diagram. We first find all the downward-pointing vertical arcs that go off the bottom of the diagram and reappear at the top, and using vertical flips, we can switch these to vertical arcs that point upward. So our diagram consists of horizontal arcs that go right to left, and vertical arcs that are either oriented upwards or downwards. Then, as mentioned in [M3], and as can be seen from the formulas in [MM], we will have that $r(K) = n - u$, where n is the braid index, and u is the number of upward pointing arcs. We will also have $tb(K) = \text{writhe}(K) - u$.

Next note that a Legendrian positive stabilization in a rectangular diagram is obtained by taking a vertical arc and putting a rectangular “kink” in it, as in the middle column in Figure 16. To then obtain a braided rectangular diagram, one performs a flip move on the left-pointing horizontal arc. This is a Legendrian isotopy, so we obtain the right-most column in Figure 16. Using the formulas above, one can see that r increases by 1, since the number of upward vertical arcs stays the same, and the braid index increases by 1. Also, tb decreases by 1, since when viewed as a braid, this Legendrian positive stabilization is a negative braid stabilization, and thus decreases the writhe by 1.

Similarly, a Legendrian negative stabilization in a rectangular diagram is obtained by taking a horizontal arc and putting a rectangular kink in it; if desired, one may perform a

flip move on the upward-pointing vertical arc. See the bottom row in Figure 16. One can see that this negative stabilization decreases r by 1, since it does not change the braid index, but introduces a new upward-pointing vertical arc. Also, tb decreases by 1, since when viewed as a braid this Legendrian negative stabilization is a braid isotopy, and thus cannot change the writhe.

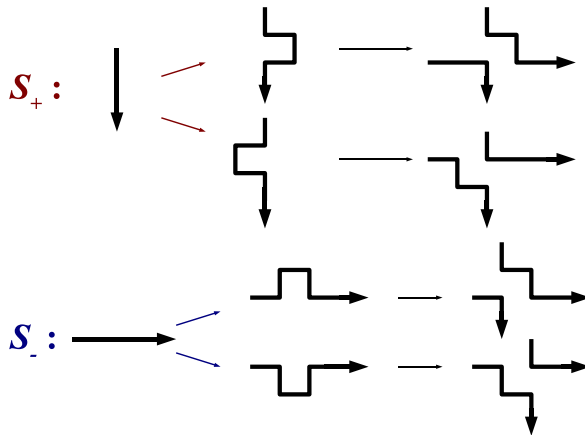


FIGURE 16. Legendrian positive and negative stabilizations in rectangular diagrams are given in the middle column. A Legendrian isotopy then yields braided rectangular diagrams in the left-most column.

As an aside, we note that by using horizontal and vertical flip moves, a rectangular diagram can be made so that all vertical arcs point downward and all horizontal arcs point to the right. In this case, the rectangular diagram is a braided rectangular diagram with two axes; one axis can be viewed as a vertical axis behind the diagram, and another can be viewed as a horizontal axis in front of the diagram. In this setting, the Legendrian positive stabilization looks like a negative braid stabilization in the vertical axis, while a Legendrian negative stabilization looks like a negative braid stabilization in the horizontal axis.

We are now in a position to look at the representatives of Legendrian isotopy classes in $\mathcal{K}_{(2,3)}$. Our beginning is L_+ . It has $tb = 5$ and $r = 2$, and we know from [EH] that its Legendrian isotopy class does not Legendrian destabilize. In the mountain range in Figure 2, this is the outer circle at $(r, tb) = (2, 5)$. We claim that the inner dot at $(r, tb) = (2, 5)$, which is $S_+(K_+)$, is represented by the braided rectangular diagram shown in [M3] obtained by performing an elementary negative flype (or negative microflype; see [BM]) to the braided rectangular diagram of L_+ . This elementary negative flype can be thought of as forcing a Legendrian positive destabilization (which looks like a negative braid destabilization in the braided diagram) that can only be performed if a Legendrian positive stabilization occurs. This results in (r, tb) still being $(2, 5)$. L_+ and the diagram after the flype are shown in Figure 17. The positive destabilization occurs on the pink arc, the stabilization on the green arc.

We now need to show that after the flype, the resulting knot Legendrian positively destabilizes after a sequence of Legendrian isotopies, thus proving that it is indeed $S_+(K_+)$. In particular, consider Figure 18. Part (a) is the knot obtained from L_+ following an elementary negative flype to the braided rectangular diagram. This knot has $(r, tb) = (2, 5)$.

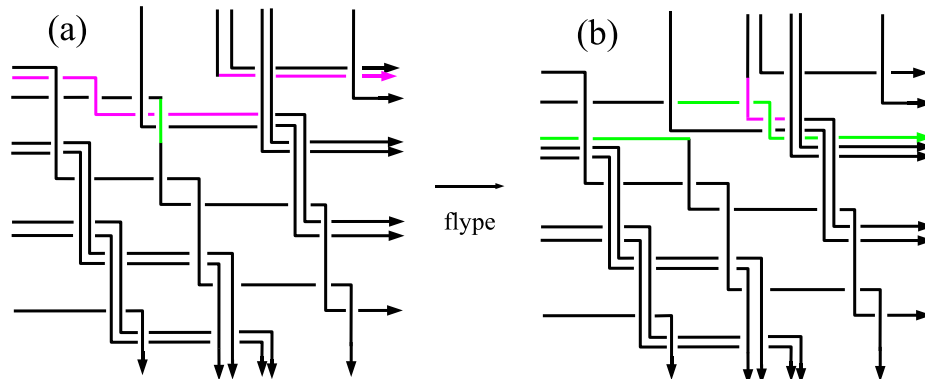


FIGURE 17. L_+ is drawn in (a). An elementary negative flype, seen as a Legendrian positive stabilization on the green arc and Legendrian positive destabilization on the pink arc, is used to obtain the knot in (b).

Indicated in (a) is a vertical arc in blue. If we move this to the right via a Legendrian isotopy, we can perform a Legendrian flip on the red horizontal arc and then slide the red horizontal arc upward over a black horizontal arc. After reversing the original flip, we obtain the knot in (b). In (b), we now focus in on the light blue and orange arcs. We can slide the light blue vertical arc to the left, and then do a Legendrian flip on the horizontal orange arc. We can then slide that horizontal orange arc down over two black horizontal arcs. After reversing the flip, we obtain (c). In (c), there is now a Legendrian positive destabilization indicated by the box in red hatching. If we perform this destabilization, we arrive at K_+ in the Legendrian mountain range in Figure 2. Taking (c) in Figure 18 and doing a Legendrian flip and some Legendrian isotopies, we obtain K_+ as drawn in Figure 19.

So the knot that we obtain after the Legendrian positive destabilization is K_+ . In principle we can then realize as a rectangular braided diagram the Legendrian isotopy class of every knot in the mountain range. For to obtain all knots with $r \geq 0$, we just need to apply a sequence of positive or negative Legendrian stabilizations to K_+ or L_+ ; to obtain the knots with $r < 0$ we just take the knots with $r > 0$ and reverse their orientation (we will justify this last statement shortly). Let us look at some relationships amongst the resulting knots.

We first consider again the two knots at $(r, tb) = (2, 5)$, namely L_+ and the resulting knot after the flype, $S_+(K_+)$. They are shown in (a) and (b) of Figure 20. Now we can Legendrian positively stabilize L_+ at the green arc in (a), and positively stabilize $S_+(K_+)$ in (b) on the pink arc. In each case, the resulting knot looks exactly the same, shown in (c). Since Legendrian stabilization does not depend upon where the stabilization occurs, this shows that $S_+(L_+)$ and $S_+^2(K_+)$ are Legendrian isotopic, as was established in [EH]. Moreover, from this figure we can also see the relationship between $S_-^k(L_+)$ and $S_-^k(S_+(K_+))$ for any k , where S_-^k indicates k consecutive Legendrian negative stabilizations. For if we perform k Legendrian negative stabilizations on the knots in (a) and (b) away from the support of the flype, we can perform them so that the rectangular diagrams of $S_-^k(L_+)$ and $S_-^k(S_+(K_+))$ differ by an elementary negative flype. Furthermore, using positive stabilizations similar to those in Figure 20, it is evident that $S_+(S_-^k(L_+))$ and $S_+(S_-^k(S_+(K_+)))$ are Legendrian isotopic.

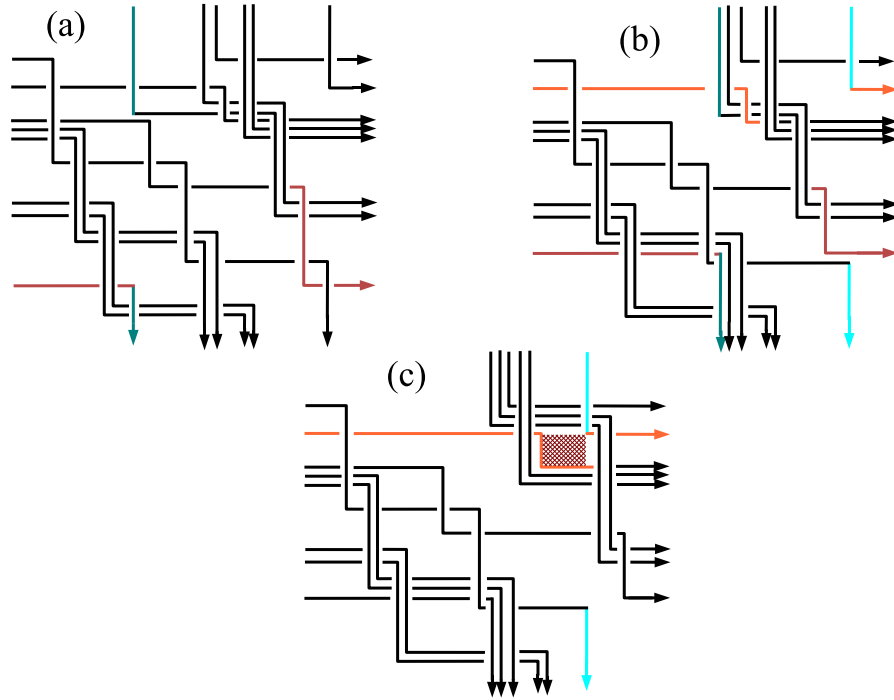


FIGURE 18. Moving from (a) to (b) to (c) can be accomplished by a sequence of Legendrian moves that reveal a Legendrian positive destabilization, indicated by the box in red hatching.

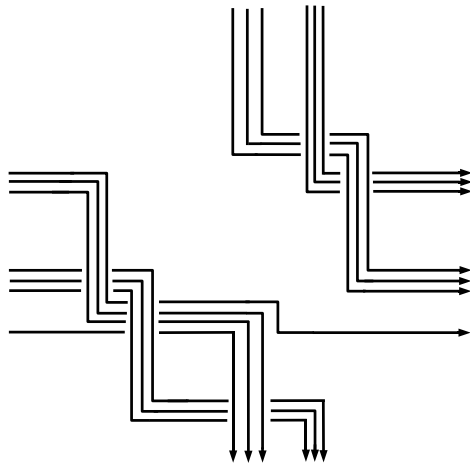


FIGURE 19. Shown is K_+ .

To continue our discussion of how to realize the Legendrian mountain range, we note that given a knot K at (r, tb) , the knot at $(-r, tb)$ can be obtained by just reversing the orientation of K . One can see this easily in the front projection in ξ_{sym} . There, the rotation number is given by $\frac{1}{2}(D - U)$, where D is the number of down cusps and U is the number of up cusps. Reversing orientation simply changes down cusps to up cusps, and vice versa, so that the new knot has rotation number $-r$. Similarly, since tb is the writhe of the front projection minus half the number of cusps, tb remains the same after reversing the orientation. This new knot is called the *Legendrian mirror* of K . To see how we can

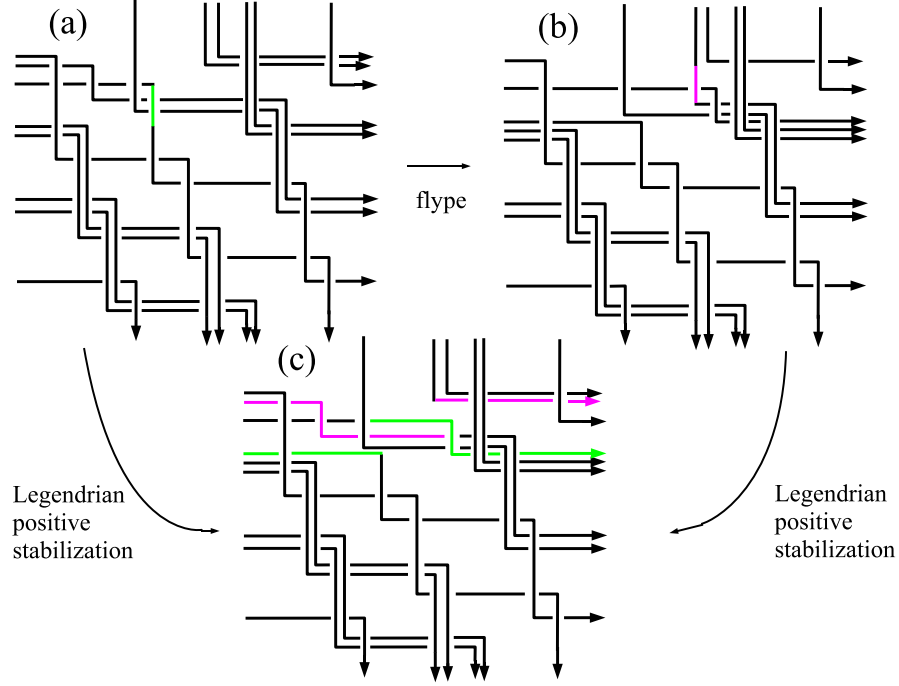


FIGURE 20. L_+ is shown in (a), and $S_+(K_+)$ in (b). Performing a Legendrian positive stabilization on each of them results in the same diagram, shown in (c). This shows that $S_+(L_+)$ and $S_+^2(K_+)$ are Legendrian isotopic.

obtain the braided rectangular diagram of this new knot, we take the braided rectangular diagram of K , and imagine it is projected onto a square. We then flip the square along the diagonal that runs from the top right to the bottom left. This is a topological isotopy of K . One then reverses the orientation, yielding vertical arcs that pass over horizontal arcs, with vertical arcs pointing down and horizontal arcs pointing to the right. This gives the braided rectangular diagram for the knot at $(-r, tb)$. In particular, we show L_- and $S_-(K_-)$ in Figure 21. To get from L_- to $S_-(K_-)$, one forces a Legendrian negative destabilization along the pink arcs, which results in an accompanying Legendrian negative stabilization along the green arc. The move from L_- to $S_-(K_-)$ is an elementary negative flype in the horizontal braid axis. A flip of the vertical arcs is a Legendrian isotopy, and so one can show as before that the knot in (b) Legendrian negatively destabilizes, and in fact is $S_-(K_-)$. Moreover, we can again see that $S_-(L_-)$ is Legendrian isotopic to $S_-^2(K_-)$, and also that $S_+^k(L_-)$ and $S_+^k(S_-(K_-))$ are related via an elementary negative flype by performing the positive stabilizations outside the support of the original flype. Furthermore, we will also have that $S_-(S_+^k(L_-))$ and $S_-(S_+^k(S_-(K_-)))$ are Legendrian isotopic.

We are now in a position to enhance the Legendrian mountain range diagram. We can again thicken the Legendrian mountain range diagram to Figure 22, where, as in Figure 4, we think of points (or circles) having coordinates (r, tb, z) . There are three planes of knots. The middle plane, which we call $z = 0$, are all the knots that arise from positive or negative Legendrian stabilization of either K_+ or K_- . These are all the central dots from the Legendrian mountain range in Figure 2. The blue lines in this plane represent Legendrian negative (de)stabilization; the red lines Legendrian positive (de)stabilization. The

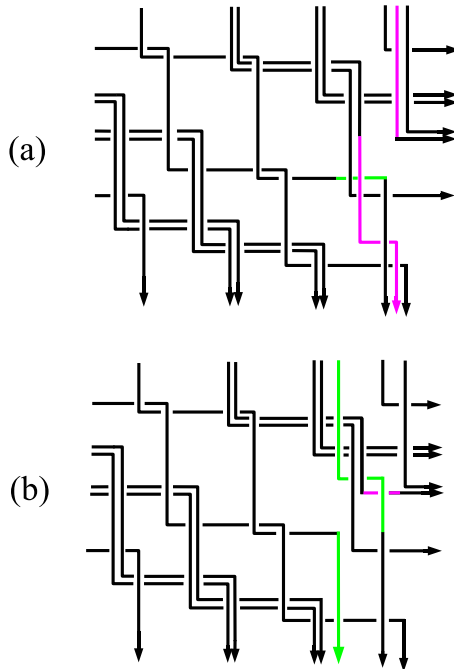


FIGURE 21. In (a) is L_- ; in (b) is $S_-(K_-)$. They are related by an elementary negative flype in the horizontal braid axis.

top plane, $z = 1$, contains L_+ and $S_-^k(L_+)$ for $k \geq 1$; these correspond to one line of circles in the mountain range in Figure 2. The green lines indicate the negative flype relating L_+ to $S_+(K_+)$ and $S_-^k(L_+)$ to $S_-^k(S_+(K_+))$. The blue lines in this plane represent Legendrian negative (de)stabilization, and the red lines going from this plane down to the plane $z = 0$ represent Legendrian positive (de)stabilization. The bottom plane, $z = -1$, contains L_- and $S_+^k(L_-)$; these correspond to the other line of circles in Figure 2. The pink lines indicate the negative flype relating L_- to $S_-(K_-)$ and $S_+^k(L_-)$ to $S_+^k(S_-(K_-))$. The red lines in this plane represent Legendrian positive (de)stabilization, and the blue lines going from this plane up to the plane $z = 0$ represent Legendrian negative (de)stabilization. As can be seen, given an arbitrary Legendrian isotopy class, we can move from that class to a class of maximal tb number without using Legendrian stabilization; moreover, Legendrian destabilizations and elementary negative flypes in braided rectangular diagrams are sufficient.

4. TRANSVERSE PUSH-OFFS AND LEGENDRIAN MOUNTAIN RANGES

In this last section, we give a pictorial classification of the transverse isotopy classes for a $(2,3)$ -cable of a $(2,3)$ -torus knots. To do this, we will be applying previous results of others to our enhanced Legendrian mountain range. To begin, given a Legendrian knot K , we can identify to it two transverse knots, called, respectively, the positive and negative transverse push-offs of K . We will call these $T_+(K)$ and $T_-(K)$, referring the reader to [E1] for more details. In fact, as mentioned in [E1], any transverse knot can be represented as a positive (or negative) push-off of a Legendrian knot. Moreover, we know that $sl(T_+(K)) = tb(K) - r(K)$. Now if we think of the enhanced Legendrian mountain range in Figure 22 as lying in 3-space with points having coordinates (r, tb, z) , then the

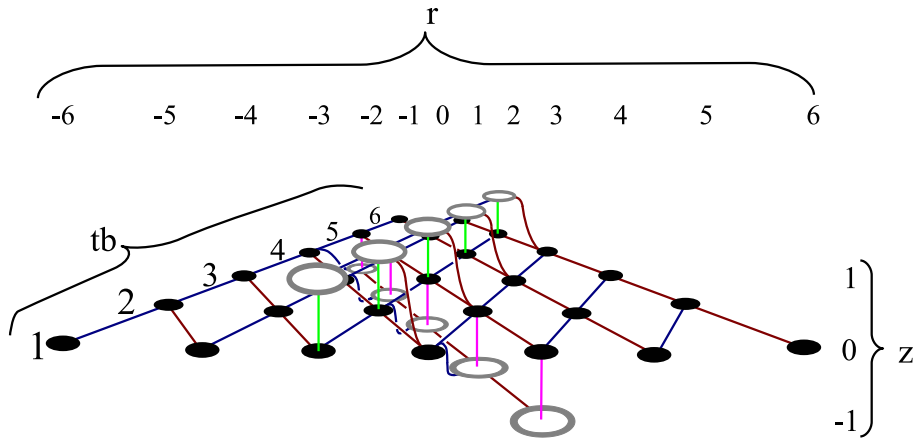


FIGURE 22. Shown is the enhanced Legendrian mountain range for a $(2, 3)$ -cable of a $(2, 3)$ -torus knot. Blue lines indicate Legendrian negative stabilization; red lines indicate Legendrian positive stabilization. The green and pink lines indicate negative flypes performed on braided rectangular diagrams in two axes.

left edge of the enhanced Legendrian mountain range is the line $tb - r = 7$. We extend this to the plane $tb - r = 7$ in 3-space, and then look at parallel translates of this plane. These will be the planes $tb - r = N$ for real numbers N , and for N an odd integer, $N \leq 7$, such planes will intersect all transverse $(2, 3)$ -cables of $(2, 3)$ -torus knots which have the same self-linking number. The following theorem relates Legendrian isotopy and transverse isotopy for Legendrian knots and their positive transverse push-offs that reside in these planes [EFM]:

Theorem 4.1 (Epstein, Fuchs, Meyer). *Let K_1 and K_2 be two Legendrian knots. Then the transverse knots $T_+(K_1)$ and $T_+(K_2)$ are transversely isotopic if and only if $S_-^m(K_1)$ and $S_-^n(K_2)$ are Legendrian isotopic for some m and n (where m and n could be zero).*

We then see that when we take positive transverse push-offs of all the Legendrian knots in Figure 22, the transverse knots in the plane $tb - r = N$, where $N \neq 3$, will all be transversally isotopic, since eventually all the Legendrian representatives of these knots Legendrian negatively stabilize to the same isotopy class. For the plane $tb - r = 3$, the transverse knots in the plane $z = 1$ are transversally isotopic to each other; also, the transverse knots in the planes $z = 0$ and $z = -1$ are all transversally isotopic to each other, since the knots in these latter two planes have Legendrian representatives that negatively stabilize to the same isotopy class. But the two transverse isotopy classes are distinct. Moreover, since the braided rectangular diagrams of transverse push-offs are the same as the diagrams for their Legendrian knots from which they came ([MM]), we know that these two transverse isotopy classes are related by an elementary negative flype. We thus obtain a diagram for the transverse isotopy classes of $\mathcal{K}_{(2,3)}$ as shown in Figure 23. The green arrow represents an elementary negative flype of braids, and the black arrows represent negative braid stabilization. It is evident that given an arbitrary transverse isotopy class, one may move toward the class with maximal sl without using stabilization; moreover, negative braid destabilizations and an elementary negative flype are sufficient.

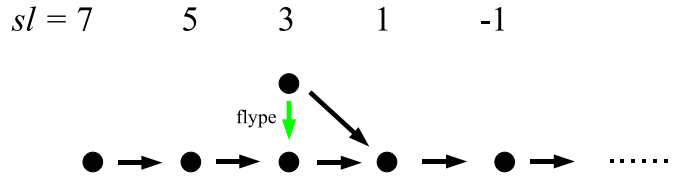


FIGURE 23. Shown are the transverse isotopy classes for a $(2,3)$ -cable of a $(2,3)$ -torus knot. The green arrow represents an elementary negative flype of braids, and the black arrows represent negative braid stabilization.

5. CONCLUSION

To put this discussion in a larger context, in [BM] the Markov Theorem without Stabilization (MTWS) was established. In a nutshell, the MTWS says that for fixed braid index n^b there are a finite number of “modeled” isotopies (dependent only on n^b) that take any oriented link represented as an n^b -braid to a representative of minimal braid index without the need for increasing the braid index. Once at minimal index there is a finite number of “modeled” isotopies (again, dependent only on the value of the index) that allow us to jump between conjugacy classes of minimal index. These isotopies (which will grow in number as n^b grows) make up the MTWS *calculus* for closed braids.

Using Legendrian braid representations to depict Legendrian classes of $\mathcal{K}_{(2,3)}$ our analysis yields a *Legendrian Markov Theorem without Stabilization* (LMTWS) for this particular knot type. The associated *Legendrian calculus* for this knot type-specific LMTWS is made up of elementary negative flypes plus positive and negative destabilizations. Here, the elementary negative flypes allow us to move toward the maximal tb value without having to use Legendrian stabilizations. This Legendrian calculus is illustrated in Figure 22 and determines an associated *transverse Markov Theorem without Stabilization* (TMTWS) illustrated in Figure 23. The *transverse calculus* for this knot type-specific TMTWS employs negative braid destabilizations and an elementary negative flype to move toward maximal self-linking number in the transverse classes of a $(2,3)$ -cable of a $(2,3)$ -torus knot.

It is of interest to see how the relationships between the MTWS, on the one hand, and the LMTWS and TMTWS on the other, extend to general knot types.

REFERENCES

- [BF] J. Birman and E. Finkelstein, *Studying surfaces via closed braids*, Journal of Knot Theory and Its Ramifications, Vol. 7, No. 3 (1998), 267-334.
- [BM] J. Birman and W. Menasco, *Stabilization in the braid groups-I: MTWS*, Geometry & Topology 10 (2006), 413-540.
- [EFM] J. Epstein, D. Fuchs, and M. Meyer, *Chekanov-Eliashberg invariants and transverse approximations of Legendrian knots*, Pac. J. Math. 201 (1) (2001), 89-106.
- [E1] J. Etnyre, Legendrian and Transversal Knots, in *Handbook of Knot Theory*, Elsevier (2005), 105-185.
- [E2] J. Etnyre, *Introductory Lectures on Contact Geometry*, Proc. Sympos. Pure Math. 71 (2003), 81-107.
- [EH] J. Etnyre and K. Honda, *Cabling and transverse simplicity*, Ann. of Math. (2) 162 (2005), no. 3, 1305-1333.
- [G] E. Giroux, *Convexité en topologie de contact*, Comm. Math. Helv. 66 (1991), 615-689.
- [H] K. Honda, *On the classification of tight contact structures I*, Geometry & Topology 4 (2000), 309-368.
- [K] Y. Kanda, *The classification of tight contact structures on the 3-torus*, Comm. in Anal. and Geom. 5 (1997), 413-438.

- [MM] H. Matsuda and W. Menasco, *On rectangular diagrams, Legendrian knots and transverse knots*, eprint at arXiv:0708.2406.
- [M1] W. Menasco, *On iterated torus knots and transversal knots*, *Geometry & Topology* 5 (2001) Paper no. 21, 651–682.
- [M2] W. Menasco, *Erratum: On iterated torus knots and transversal knots*, *Geometry & Topology* 5 (2001), 651–682, eprint at arXiv, math.GT/0610565.
- [M3] W. Menasco, *An addendum on iterated torus knots*, eprint at arXiv, math.GT/0610566.